

Theoretical Approach to Estimate Intermodulations in Wideband Active Transmit Phase-Array Antennas

EHSAN JOHARI,¹ HALEH KARKHANEH,¹ and
AYAZ GHORBANI¹

¹Department of Electrical Engineering, Amirkabir University of Technology,
Tehran, Iran

Abstract *In this article, an active phased-array multi-beam antenna model including the nonlinear model of the amplifier is developed and validated by experimental data. An amplifier model with frequency-dependent parameters is considered. To investigate nonlinearity effects in a phased-array antenna, a two-beam S-band array is analyzed, and the results of the proposed method are compared with measured data. It is shown that the presented model is able to precisely predict the intermodulation products with an accuracy of 1 dB. Therefore, the model can be used as a tool to accurately predict the intermodulation patterns for multi-beam satellite array applications, avoiding excessive system margin and reducing DC power consumption.*

Keywords active phase-array antennas, nonlinear distortion, intermodulations, memory effects

1. Introduction

In the last 20 years, the attitude of antenna theory and technology has changed, and one important cause of this change is active antennas, especially active-array antennas. Integration of active circuitry with antennas has many advantages over conventional passive antennas, e.g., increasing the effective length of a short antenna, increasing the bandwidth, decreasing the mutual coupling between array elements, and improving the noise factor (Loyka & Mosig, 1999). Also future satellite communication payloads require high directivity and multiple beams with large signal bandwidth to satisfy broad-band applications, such as multimedia and voice conferences. Therefore, an active phased array is ideal for such applications, since they can be configured in orbit to provide the bandwidth in demand and increase overall system utilization (Maalouf & Lier, 2004; Hemmi, 2002). The total transmission quality of a communication satellite using a multi-beam phased-array antenna system is most dependent upon the nonlinear distortion of the solid state power amplifier (SSPA) modules (Loyka & Mosig, 1999; Kohls et al., 1995). This distortion brings about intermodulation (IM) interferences. The closer to the compression point due to the most power efficiency means more IM product levels that degrade carrier-to-interference ratio (C/I) associated with beam steering direction. So, accurate modeling of these IM beams helps control the IM interference, thus allowing

Received 22 April 2011; accepted 25 September 2011.

Address correspondence to Haleh Karkhaneh, Department of Electrical Engineering, Amirkabir University of Technology, No. 424, Hafez Ave., Tehran, Iran. E-mail: h_karkhane@aut.ac.ir

the SSPAs to be operated with minimum back-off since fewer margins are needed. This results in a more efficient array that requires a lower system DC power with reduced mass and cost of the satellite (Maalouf & Lier, 2004).

Intermodulation products (IMPs) in an active-array antenna have characteristics that are different from those in lumped active circuits and systems. For multiple-beam satellite digital communication systems, signal suppression and IMP interference in amplifiers may degrade the bit-error rate 1 to 5 dB in comparison to passive antennas. The presence of interfering signals may result in an increase of the array beam-width, side-lobe level, null depth degradation, as well as changing the null positions (Loyka & Mosig, 1999). A block diagram of an active phased-array transmit antenna is illustrated in Figure 1. It consists of K radiating antennas, K SSPAs, and N carrier signals that have different amplitudes and phases.

Sandrin (1973) previously analyzed the radiating patterns of third- and fifth-order IM products of active arrays. In his analysis, he derived the phase gradient for the m th-order

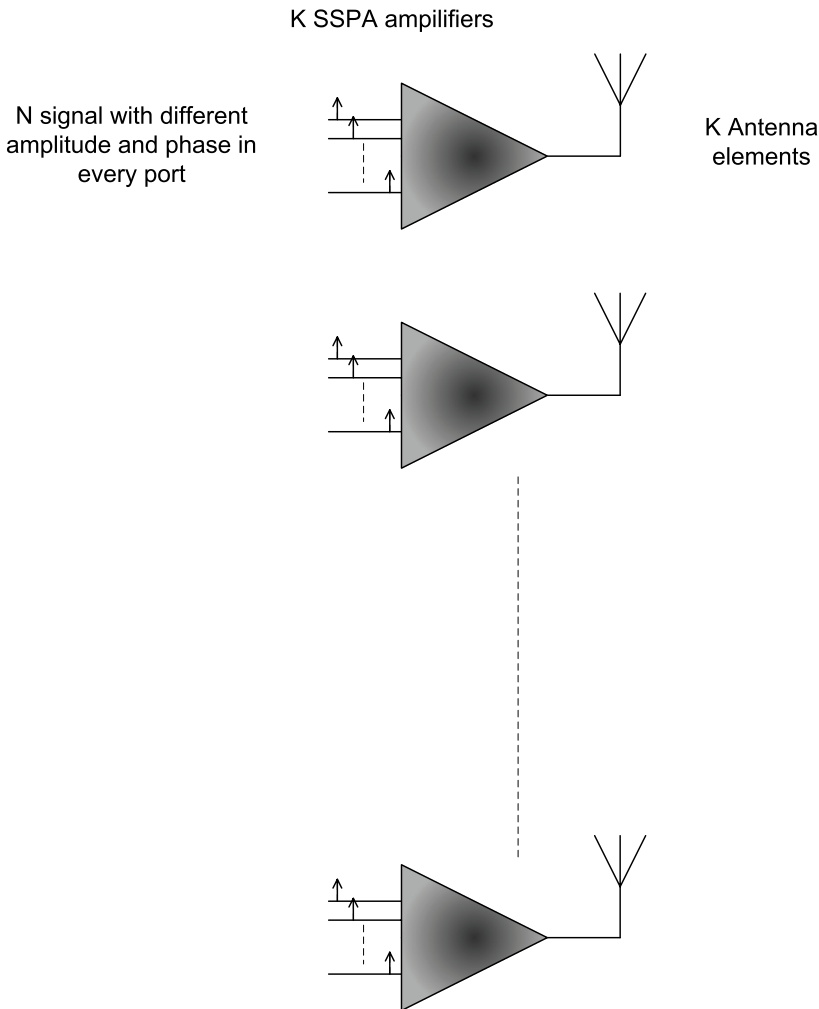


Figure 1. Block diagram of an active phased-array transmit antenna.

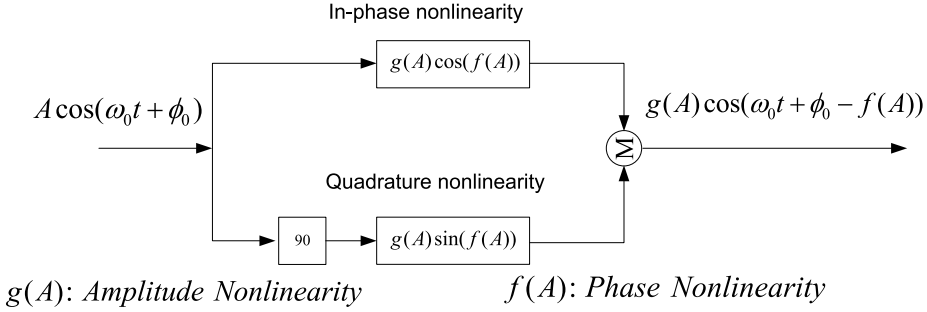


Figure 2. Frequency-independent nonlinear quadrature model.

intermodes and used generic transfer functions for a nonlinear amplifier. His analysis incorporates approximations appropriate for limited field of view arrays (as in the case of an earth-looking antenna on a geosynchronous satellite) and for small percentage bandwidth. Kohls et al. (1995) presented simulation and experimental results for KU-band arrays. They used a Bessel series to fit the above-mentioned model of a KU-band array for predicting third-order IM product beam patterns. Meanwhile, Maalouf and Lier (2004) studied IM estimation in an active phased-array theoretically and experimentally.

All of these studies involved narrow band signals. The frequency-independent nonlinear quadrature model of Figure 2 is widely used for modeling amplifiers exhibiting both AM/AM and AM/PM conversion. This implies that the amplifier characteristics are frequency independent over the frequency band of interest. However, while having broadband input signals, or systems including wide-band amplifiers and relatively narrow-band components, a frequency-dependent quadrature model is required (Abuelma'atti, 1984).

This article consists of six sections. In Section 2, power amplifiers (PAs) are modeled. Then, the mathematical modeling of IM products is calculated in Section 3. Next, the alternative frequency-dependent model is used in Section 4, and finally, the radiation far-field pattern is considered in Section 5. The measured and simulated results are presented in Section 6, and conclusions are given in Section 7.

2. Nonlinear SSPA models

The main idea of quadrature modeling technique is using a complex envelope instead of real narrow band signals; thus, there is no carrier information in the complex envelope except the modulation information. This point is important from the viewpoint of computational efficiency. The SSPA characteristics are modeled with series of Bessel function coefficients because of their ability to quickly converge to the nonlinear characteristics of the amplifier and model the IM products at the output of the amplifier. The mathematical model provides the gain and phase insertion of each carrier and IM component at the output of the SSPA; therefore, it is suitable to incorporate into the antenna phased-array model. Therefore this method can achieve the necessary accuracy for active phased-array systems (Shimbo, 1971; Vuong & Henchey, 1981). The nonlinear behavior of the amplifier can be expressed by the following Bessel function series:

$$g(A)e^{jf(A)} = \sum_{s=1}^S \beta_s J_1(\alpha_s A), \quad (1)$$

where A , $g(A)$, and $f(A)$ denote the amplitude of the input tone and measured AM/AM and AM/PM single-tone characteristics, respectively. J_1 is the Bessel function of the first kind with order 1; β_s , α , and S are the complex number, the real number, and an integer, respectively. The appendix in Vuong and Henchey (1981) shows in detail how the parameters S and α are chosen to evaluate β_s by the linear search method. A typical value for the integer S is less than 20, while α is selected such that $1 < \alpha$. $A_{sat} < 2$, where A_{sat} is the saturation voltage of the amplifier. Once S and α are selected, β_s are calculated to separately satisfy the real and imaginary part of Eq. (1). In particular, the solution to the following two equations uses the least-squares method (Vuong & Henchey, 1981) as

$$\begin{aligned} \min_{\beta_{real}} & \left| \sum_{i=1}^P g(A_i) \cos(f(A_i)) - \sum_{s=1}^S \beta_{real} J_1(\alpha s A_i) \right|^2, \\ \min_{\beta_{imag}} & \left| \sum_{i=1}^P g(A_i) \sin(f(A_i)) - \sum_{s=1}^S \beta_{imag} J_1(\alpha s A_i) \right|^2. \end{aligned} \quad (2)$$

Here, P is the number of measured sample points during the characterization of the AM/AM and AM/PM behavior of the amplifier. With S and α fixed, both equations in Eq. (2) are quadratic minimization problems in $\beta_{real}(s)$ and $j\beta_{imag}(s)$ with known analytical solutions. Next, Eq. (2) is solved for several (S, α) pairs, and the solution with the lowest residual error is kept. The final model coefficients are given by $\beta(s) = \beta_{real}(s) + j\beta_{imag}(s)$.

3. IM Modeling

This section investigates the effects of IM upon the performance of a K -element planar phased-array antenna satellite communication system. In an array, the input signal of the k th amplifier of the array can be represented by

$$e(k, t) = \sum_{n=1}^N A_{nk} e^{i(2\pi f_n t + \phi_{nk})}, \quad (3)$$

where A_{nk} is the amplitude of the n th channel at the k th element, which, in this work, is assumed constant over time; t , ϕ_{nk} is the corresponding phase, and f_n is the carrier frequency at the given channel. At the output of the amplifier, the signal is composed of the amplified carriers and IM components that are introduced by the nonlinear amplifier characteristics (Maalouf & Lier, 2004). The output signal is expressed as

$$e_o(k, t) = \sum_{L_P} M(L_P) e^{i \sum_{n=1}^N l_n (2\pi f_n t + \phi_{nk})}, \quad (4)$$

where L_P is a vector member of the set

$$L = \left\{ \{l_1, l_2, \dots, l_N\}, \sum_{n=1}^N l_n = 1, \text{ and } \sum_{n=1}^N |l_n| = 1 \text{ or } 3 \right\} \quad (\text{Maalouf \& Lier, 2004}), \quad (5)$$

where the components that correspond to $\sum_{n=1}^N |l_n| = 1$ are carriers, and the components that correspond to $\sum_{n=1}^N |l_n| = 3$ are third-order IM products. For each index p , there is a unique set of integer number l_1 to l_n . In addition, higher-order products are ignored because they are lower than the third order, at least 6 dB (Maalouf & Lier, 2004). Furthermore, the voltage gain of the p th component $M(L_p)$ is derived in Vuong and Henchey (1981), and can be expressed as

$$M(L_p) = \sum_{s=1}^S \beta_s \prod_{n=1}^N J_{l_n}(\alpha A_{nk} s). \quad (6)$$

4. Frequency Dependency

Most amplifiers exhibit frequency-dependent amplitude nonlinearity and AM/PM conversion characteristics. Therefore, using the minimum mean square error curve-fitting procedure, a quadrature model can be derived for each input frequency. This would result in the frequency-dependent parameters $\beta_s(f)$, $s = 1, \dots, S$ as

$$\beta_s(f) = \beta_{0s} \cdot G_s(f), \quad s = 1, \dots, S, \quad (7)$$

where β_{0s} is the frequency-independent parameter, and $G_s(f)$ is the function of frequency f . So, the frequency-independent quadrature model of Figure 2 can be modified to fit the frequency-dependent quadrature model as well, as illustrated in Figure 3. Each dependent envelope nonlinearity has $\beta_{0s} J_1(\alpha A s)$, and the output amplitudes are scaled by the filter $G_s(f)$.

Therefore, a multi-tone input signal with arbitrary tone amplitudes is processed by several parallel connected branches. Each branch consists of a frequency-independent amplitude nonlinearity followed by an appropriate filter. For instance, at the output of frequency-independent nonlinearity $\beta_{0s} J_1(\alpha A s)$, a wide range of products are produced, and by using Eq. (6), the amplitude of the output product is given by $\beta_s \prod_{n=1}^N J_{l_n}(\alpha A_{nk} s)$. Next, due to the filter action, this value is scaled by the amount $G_s(f)$. Therefore, the

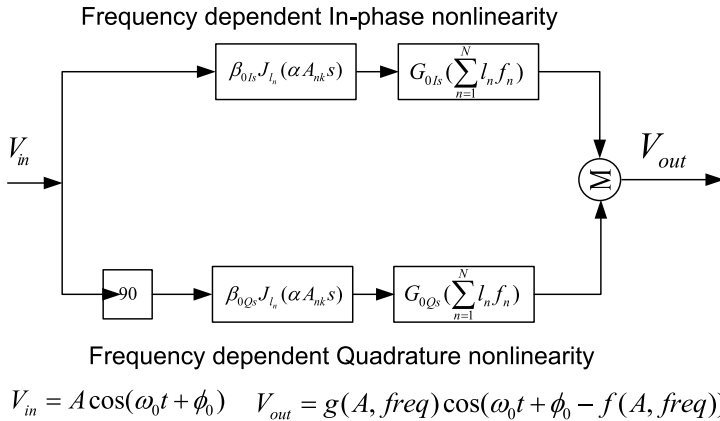


Figure 3. Frequency-dependent quadrature model.

amplitude of the output product will be given by

$$M(L_p) = \sum_{s=1}^S \beta_s \prod_{n=1}^N J_{l_n}(\alpha A_{nk} s) \cdot G_{0s} \left(\sum_{n=1}^N l_n f_n \right). \quad (8)$$

5. Radiating Array Model

The radiation pattern of the array is modeled analytically as the product of the element pattern and the array factor, assuming identical element patterns over the array and no mutual coupling. These assumptions are relatively accurate for patch elements with distances of 1.5 times greater than lambda, which are considered in the modeling. Furthermore, it is assumed that the fundamental TM10 mode is propagating in the microstrip patch antenna. Here, the radiating elements are modeled in an array environment, and the array factor's far-field array factor radiation patterns are calculated for both the carriers and IM products based on excitation coefficients generated by the IM algorithm. The far-field array factor radiation pattern $P_p(\theta)$ for each component in any spatial direction is given by the coherent sum of the corresponding SSPA output component given in Eq. (8), expressed as

$$P_p(\theta) = M(L_p) \times \sum_{k=1}^K \left\{ \exp i \frac{2\pi}{\lambda_p} (\cos \phi_n x_k + \sin \phi_n y_k) \sin \theta_n \cdot \exp i \sum_{n=1}^N l_n \phi_{nk} \right\}, \quad (9)$$

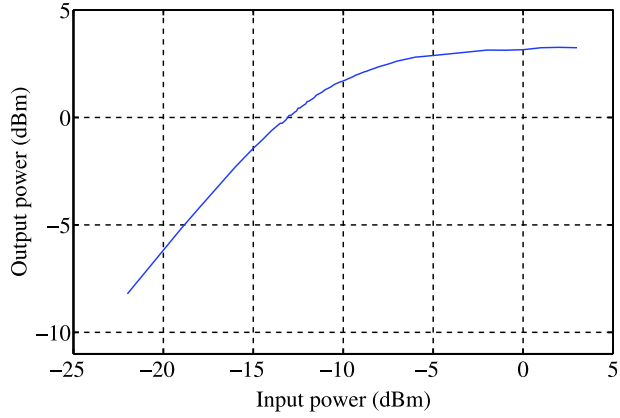
where λ_p is the wavelength of the p th component whose frequency is given by $\sum_{n=1}^N l_n f_n$, (x_k, y_k) are the Cartesian coordinates of the array elements, and (θ_n, ϕ_n) defines the spatial beam directions in spherical coordinates for the n th beam (Maalouf & Lier, 2004).

6. Results

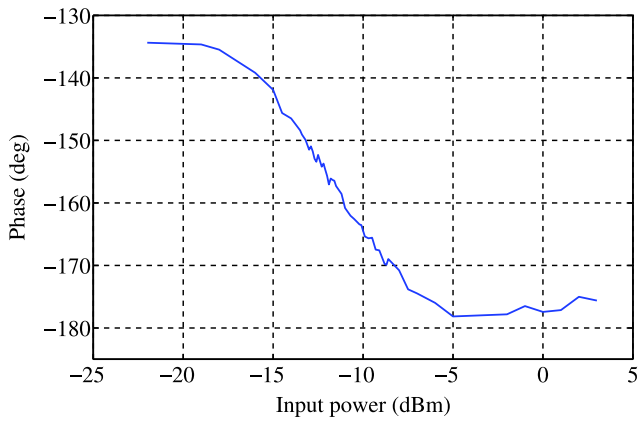
In this article, a two-beam S -band array has been studied, which is comprised of eight patch antenna elements in a $1 * 8$ configuration. The patch size is $2.6 \text{ cm} * 2.1 \text{ cm} * 0.32 \text{ cm}$, and the substrate material is RT5880 (The Roger's Company Headquarters, Mentor, Ohio, USA). The amplifier characterization is described by measuring the single-tone AM/AM and AM/PM of a subset of the SSPA with a frequency of 3.5 GHz to represent the nonlinear response of the element, as shown in Figure 4.

Then, the amplifier is modeled as described in Section 2 with seven terms of Bessel functions. To demonstrate the accuracy of the proposed model, the two-tone power sweep experimentation at the P1 dB point has been done and compared with the modeling results. Figure 5 illustrates the results of the two-tone power sweep test with $f_1 = 3,500 \text{ MHz}$ and $f_2 = 3,525 \text{ MHz}$, which includes the measured and predicted third-order IM (upper frequency) with and without frequency dependency. The agreement between the measured and predicted IM component is better than 1 dB, both in the linear region and in the compressed region for frequency-dependent model, while it is higher, about 3 dB, in the other.

After PA modeling, the array is fed by two different tones with certain tone spacing, and two beams are steered in $+20^\circ$ and -10° , in which the two cases were analyzed. In case 1, the power is set at 9 dB total power input back-off (IBO) to represent the linear operation. In case 2, the power was set at 0 dB total IBO to exhibit the compressed region. Figure 6 shows two graphs, each consisting of the zero elevation pattern cuts



(a)



(b)

Figure 4. Measured single-tone AM/AM and AM/PM of SSPA. (color figure available online)

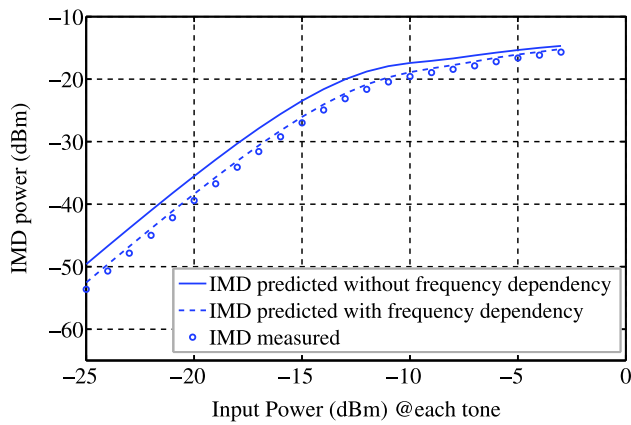
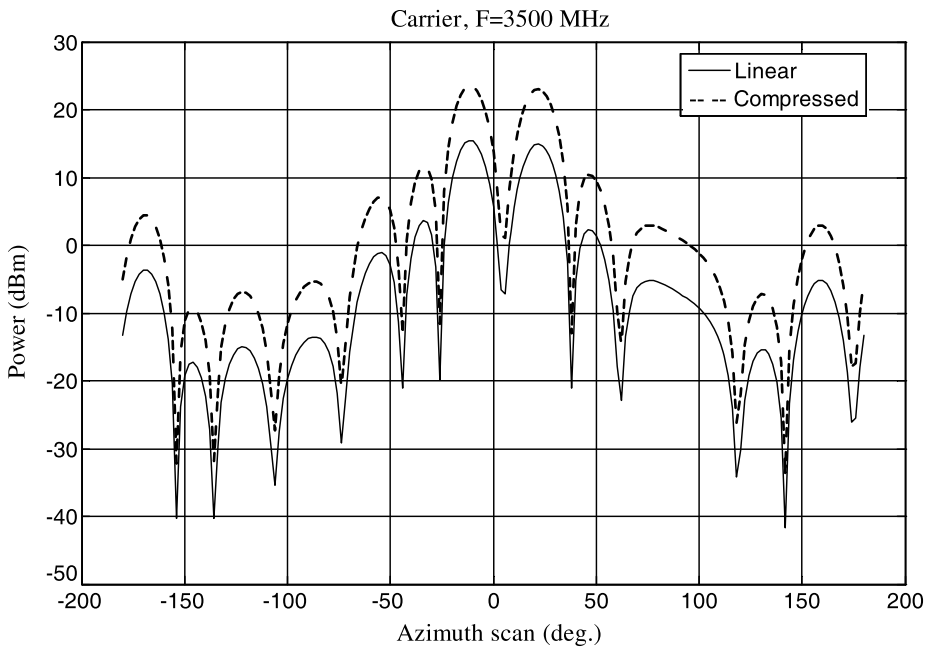
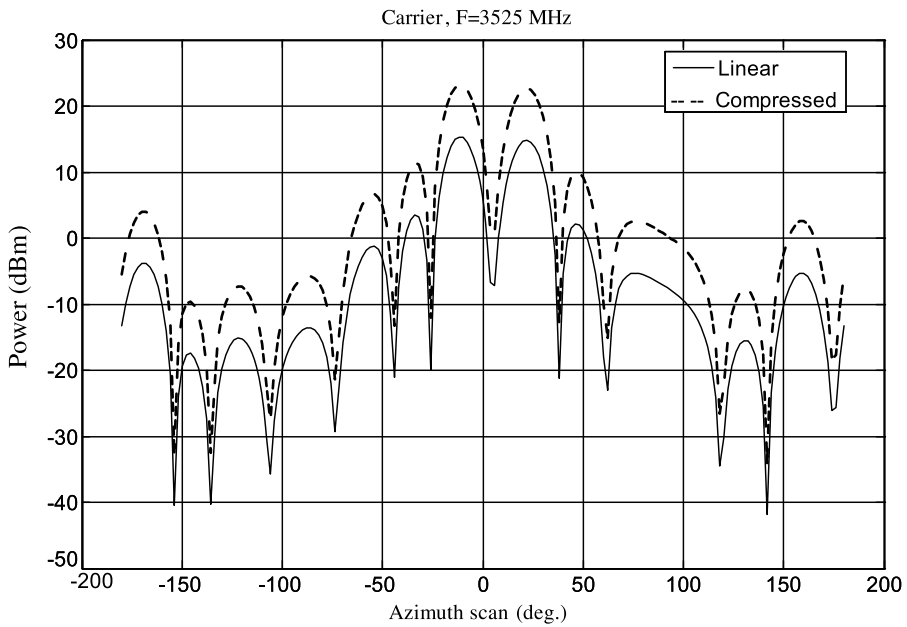


Figure 5. Two-tone validation of the SSPA model. (color figure available online)



(a)



(b)

Figure 6. Zero elevation pattern cut for two-beam steering angle of two carriers frequency at -9 dB and 0 dB IBO.

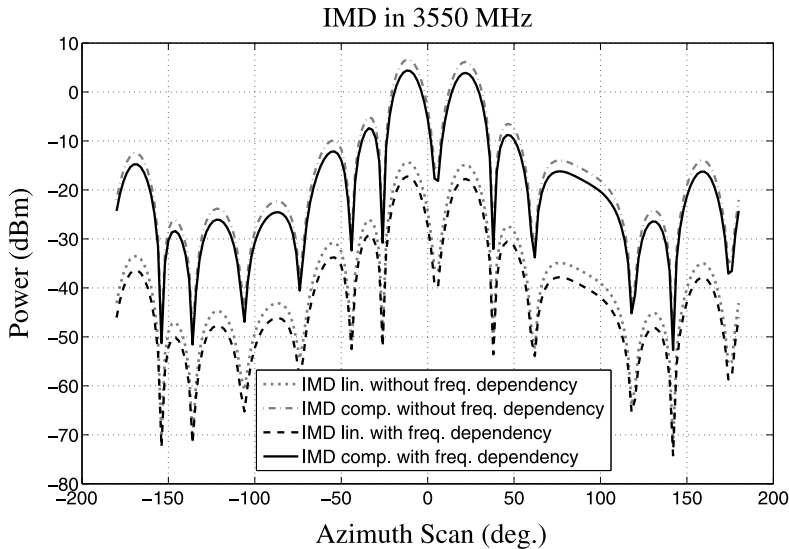


Figure 7. Zero elevation intermodulation distortion (IMD) pattern cut generated by the same carriers as in Figure 6.

of predicted carrier components in the linear and compressed region for two different steering angles. The frequency selected for each scan is given on each graph.

Figure 7 displays the predicted results of the third-order IM patterns in the frequency of 3,550 MHz for the same steering angles. The figure contains a set of four patterns, including predicted IM patterns with and without frequency dependency in the linear and the compressed region. The IMP patterns corresponding to the linear region because of the IBO have low power. The accuracy of the amplitude prediction as the result of the frequency-dependency effect is typical and has a discrepancy of about 2 dB in the peaks.

Figure 8 shows the predicted two carriers on the same graph, as well as the third-order IM component with and without frequency dependency when the array is operated at 0 dB IBO. The predicted total IM power generated by the array model without frequency dependency is about 2 dB higher than when the frequency behavior is considered. The carrier to total IM power ratio at the array far field was about 16 dB. In the accurate modeling with frequency dependency, however, the ratio is increased to about 18 dB, as seen in Figure 8. This 2-dB improvement is very efficient in controlling C/I in a multi-beam array.

7. Conclusion

A main goal in an active transmitter array is to drive the amplifiers to be as saturated as possible (for optimal efficiency) and still meet the total C/I requirement. In this article, an eight-element S-band array is simulated by the Shimbo nonlinear frequency-dependent amplifier model. The PA characteristic predictions are confirmed by measurement data. Also, the array far-field parameters, side lobe, and IM patterns are calculated in this article. This analysis presents that interference can be predicted accurately and theoretically controlled in multi-beam phased-array satellite system. Hence, it reduces the necessary

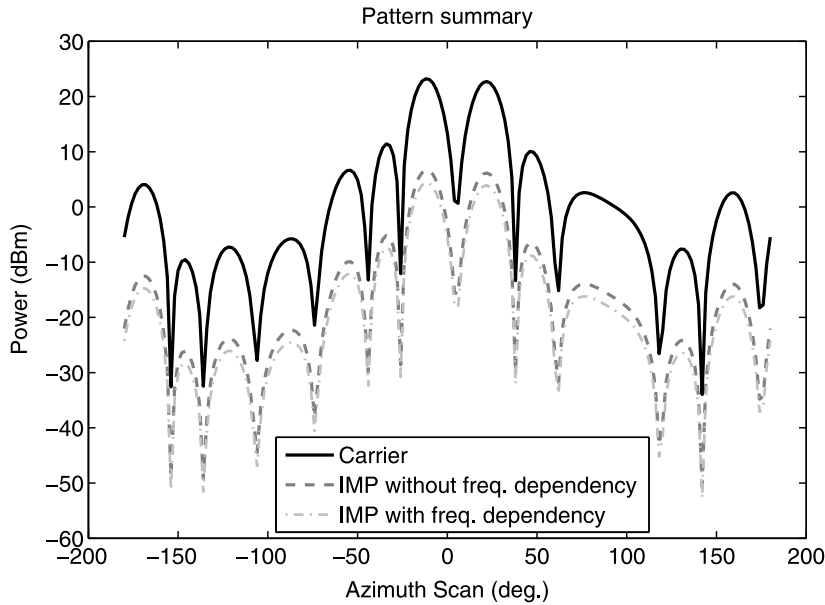


Figure 8. Predicted carrier and third-order IM power with and without frequency dependency.

excessive margin. Therefore, with this reduction, transmitter power consumption will be decreased, and consequently, satellite consumption and mass will be reduced.

References

- Abuelma'atti, M. T. 1984. Frequency dependent nonlinear quadrature model for TWT amplifiers. *IEEE Trans. Commun.* COM-32:982–986.
- Hemmi, C. 2002. Pattern characteristics of harmonic and intermodulation products in broad-band active transmit arrays. *IEEE Trans. Antennas Propagat.* 50:858–865.
- Kohls, E. C., E. P. Ekelman, A. I. Zaghoul, & F. T. Assal. 1995. Intermodulation and bit-error ratio performance of KU-band multi-beam high-power phased array. *Proc. Antennas Propagat. Soc. Int. Symp. Dig.* 3:1404–1408.
- Loyka, S. L., & J. R. Mosig. 1999. Nonlinear modeling and simulation of active array antennas. *COST Action 260*, Wroclaw, Poland, 30 June–2 July.
- Maalouf, K. J., & E. Lier. 2004. Theoretical and experimental study of interference in multi beam active phased array transmit antenna for satellite communications. *IEEE Trans. Antennas Propagat.* AP-52:587–592.
- Sandrin, W. A. 1973. Spatial distribution of intermodulation products in active phased array antennas. *IEEE Trans. Antennas Propagat.* AP-21:864–868.
- Shimbo, O. 1971. Effects of intermodulation, AM-PM conversion, and additive noise in multicarrier TWT systems. *Proc. IEEE* 59:230–238.
- Vuong, X. T., & M. A. Henchey. 1981. On the accuracy of the Shimbo approach to intermodulation and crosstalk calculations. *IEEE Trans. Commun.* COM-29:1076–1082.

Copyright of Electromagnetics is the property of Taylor & Francis Ltd and its content may not be copied or emailed to multiple sites or posted to a listserv without the copyright holder's express written permission. However, users may print, download, or email articles for individual use.